Magnetic microwires for sensor applications

Arcady Zhukov[1, 2, 3]*, Paula Corte-León[1, 2], Lorena González-Legarreta[1], Mihail Ipatov[1, 2], Ahmed Talaat[1, 2], Juan M. Blanco[2], Julian Gonzalez[1], Valentina Zhukova[1, 2]

[1]*Dpto. Fisica de Materiales, Fac. Quimicas, UPV/EHU, Paseo Manuel Lardizabal, 3, San Sebastian, 20018, Spain*
[2]*Dpto. de Física Aplicada, EIG, UPV/EHU, San Sebastian, Europa Plaza, 1,20018, Spain*
[3]*IKERBASQUE, Basque Foundation for Science, Bilbao, 48011, Spain*

*Corresponding author: Tel: (+34) 943018611; E-mail: arkadi.joukov@ehu.es

DOI: 10.5185/amlett.2019.2202
www.vbripress.com/aml

Abstract

The impact of post-processing on soft magnetic properties and the giant magnetoimpedance (GMI) effect of Fe- and Co-based glass-coated microwires is evaluated. A remarkable improvement of magnetic softness and GMI effect is observed in Fe-rich glass-coated microwires subjected to stress annealing. Frequency dependence of GMI ratio of stress-annealed Fe-rich microwires has been discussed considering frequency dependence of the skin penetration depth, δ, as well as magnetic anisotropy distribution within the metallic nucleus. Annealed and stress-annealed Co-rich microwires present rectangular hysteresis loop and single and fast domain wall propagation. However, Co-based stress-annealed microwires present high magnetoimpedance ratio. Observed stress-induced anisotropy and related changes of magnetic properties are discussed considering internal stresses relaxation and "back-stresses". Copyright © 2019 VBRI Press.

Keywords: Magnetic microwires, GMI effect, domain wall propagation, magnetic anisotropy, internal stresses.

Introduction

Soft magnetic wires can present magnetic properties suitable for industrial applications such as the giant magnetoimpedance (GMI) effect or magnetic bistability related to the large and single Barkhausen jump [**1-9**].

These properties can be observed either in crystalline or in amorphous magnetic wires, but amorphous magnetic wires present several advantages, such as superior mechanical properties, the absence of the microstructure defects (grain boundaries, crystalline texture, dislocations, point defects,…) [**6, 10**] and therefore long and precise post-processing is not required. For these reasons, amorphous wires have attracted considerable attention since the 70-s [**2-10**].

Glass-coated magnetic microwires prepared using the Taylor-Ulitovsky technique with thin metallic nucleus (typically with diameters from 0.5 to 50 μm) covered by flexible, insulating and biocompatible glass are quite demanded for a great number of applications [**8, 9, 11-16**]. The Taylor-Ulitovsky method for glass-coated microwires preparation is known since the 60-s [**17**]. This technique allows preparation of the thinnest rapidly quenched magnetic wires.

In amorphous materials the magnetocrystalline anisotropy is absent. Therefore, the magnetoelastic anisotropy becomes one of the most important parameters that determine the magnetic properties of amorphous magnetic materials [**6, 18-20**].
The magnetoelastic anisotropy, K_{me}, is given as [**21**]:

$$K_{me} = 3/2\lambda_S\sigma_i \quad (1)$$

where λ_S is the magnetostriction coefficient and σ_i is the internal stresses value.

In the case of glass-coated microwires the magnetoelastic anisotropy contribution is even more relevant since the preparation process involves not only the rapid quenching itself, but also simultaneous solidification of the metallic nucleus surrounded by the glass-coating with rather different thermal expansion coefficients [**6, 2, 22, 23**]. The strength of internal stresses, σ_i, is basically affected by the three main factors: i) quenching stresses associated to the melt quenching of the metallic alloy; ii) stresses related to the different thermal expansion coefficients of metallic ingot and glass simultaneously solidifying and iii) stresses associated to the drawing of solidifying wire [**22-24**].

Consequently, as regarding magnetic properties the as-prepared microwires are usually classified into three main groups:

- Fe-based microwires with positive ($\lambda_s \approx 10^{-5}$) λ_s -values presenting spontaneous magnetic bistability (rectangular hysteresis loop);
- Co-based wires with negative ($\lambda_s \approx -10^{-6}$) λ_s -values exhibiting almost non-hysteretic linear magnetization curves with rather high magnetic anisotropy field;
- Co-based wires with vanishing λ_s –values ($\lambda_s \approx -10^{-7}$) presenting best magnetic softness [**6**].

Fe-rich glass-coated microwires usually present the magnetic bistability effect and hence fast magnetization

switching by rapid domain wall (DW) propagation [**6**]. However, Fe-based microwires are less-expensive and present a number of advantages, i.e. higher saturation magnetization [**6**]. Additionally, Co belongs to critical raw materials [**25**]. As a consequence, the insecure supplies of Co could hinder the development of new technologies related to massive applications. Accordingly, Fe-based microwires are preferable for large scale applications. But generally as-prepared Fe-rich microwires present much lower GMI effect than Co-rich microwires [**6**].

Therefore, certain efforts have been paid to optimization of the magnetic softness and GMI effect in Fe-rich microwires [**26-29**]. One of the routes for GMI effect improvement of Fe-rich microwires consists of devitrification of amorphous precursor allowing drastic decreasing of the magnetostriction coefficient [**26, 27**]. But the disadvantage of nanocrystalline materials is poorer mechanical properties limiting possible applications.

The alternative route is the development of the induced transverse magnetic anisotropy by specially designed annealing allowing keeping the amorphous structure and hence maintaining superior mechanical properties. Recently, we demonstrated that the magnetic anisotropy induced by stress-annealing with transverse easy magnetization direction is beneficial for improvement of magnetic softness and GMI ratio **[6, 19, 28-32**].

It is worth mentioning that the main technological interest in soft magnetic wires is related to the GMI effect for which high circumferential magnetic permeability observed in properly processed magnetic wires is essentially important. The GMI effect provides excellent opportunity for design of magnetic sensors and magnetometers owing to extremely high magnetic field sensitivity (few hundred percent change of impedance under low external magnetic field reported for amorphous wires) [**5-8, 11-13, 31**].

The GMI effect is usually characterized by the GMI ratio, $\Delta Z/Z$, defined as:

$$\Delta Z/Z = [Z(H) - Z(H_{max})]/Z(H_{max}) \quad (2)$$

where H_{max} is the maximum applied DC magnetic field.

The origin of the GMI is commonly attributed to the classical skin effect of magnetic conductor [**2, 3, 20**].

Up to now the highest GMI ratio is reported for Co-rich glass-coated microwires with nearly-zero magnetostriction coefficient [**20, 21**]. Thin glass-coated microwires prepared by so-called Taylor-Ulitovsky method with typical metallic nucleus diameters of the order of a few μm are one of the most promising materials for creation of magnetic sensors and magnetometers.

Consequently, in this paper we present our recent experimental results on post- processing of magnetic microwires with aim to achieve better magnetic softness and GMI effect.

Experimental

Materials / chemicals details

We selected typical Fe-rich ($Fe_{75}B_9Si_{12}C_4$) and Co-rich ($Co_{69.2}Fe_{4.1}B_{11.8}Si_{13.8}C_{1.1}$) alloys in which the phase diagram presents deep eutectic. Such chemical compositions were used previously for preparation of amorphous Fe-rich and Co-rich microwires [**6**].

Material synthesis / reactions

Glass-coated $Fe_{75}B_9Si_{12}C_4$ (metallic nucleus diameter, d=15.2 μm, total diameter, D=17.2 μm) and $Co_{69.2}Fe_{4.1}B_{11.8}Si_{13.8}C_{1.1}$ (d=25.6 μm, D=30.2 μm) microwires with positive and low negative magnetostriction coefficients, λ_s, respectively have been prepared by Taylor-Ulitovsky technique described elsewhere [**6, 20, 21**].

Samples annealing has been performed in a conventional furnace.

The tensile stress has been applied during the annealing as well as during the sample cooling with the furnace. The mechanical load has been attached to the microwire during the annealing and slow cooling with the furnace.

The stress value during the annealing within the metallic nucleus and glass shell has been evaluated as described earlier [**28, 30**]:

$$\sigma_m = \frac{K.P}{K\ S_m + S_{gl}}, \quad \sigma_{gl} = \frac{P}{K\ S_m + S_{gl}} \quad (3)$$

where, $K = E_2/E_1$, E_i are the Young's moduli of the metal (E_2) and the glass (E_1) at room temperature, P is the applied mechanical load, and S_m and S_{gl} are the cross sections of the metallic nucleus and glass coating respectively.

Characterizations / response measurements

Hysteresis loops have been measured using fluxmetric method previously described elsewhere [**21, 23**]. We represent the normalized magnetization, M/M_0 versus magnetic field, H, where M is the magnetic moment at given magnetic field and M_0 is the magnetic moment of the sample at the maximum magnetic field amplitude, H_m.

For GMI characterization we used GMI ratio, $\Delta Z/Z$, defined by eq. (2).

As previously described [**32**], we used micro-strip sample holder placed inside a sufficiently long solenoid that creates a homogeneous magnetic field, H. The sample impedance, Z, was measured using vector network analyzer from the reflection coefficient S_{11} using expression [**32**]:

$$Z = Z_0(1 + S_{11})/(1 - S_{11}) \quad (4)$$

where, Z_0=50 Ohm is the characteristic impedance of the coaxial line. Employed GMI measurements method allows evaluation of the GMI effect in extended frequency, f, range up to GHz frequencies.

For GMI characterization we used GMI ratio defined by eq. (2).

The DW velocity, *v*, was evaluated using modified Sixtus-Tonks-like setup described elsewhere [**4**]. In this setup 3 pick-up coils are mounted along the microwire placed inside the long solenoid allowing measurement of the DW velocity at different external magnetic field [**4**].

The propagating DW induces electromotive force (*emf*) in the coils which are picked up by the digital oscilloscope. Then, the DW velocity is estimated as:

$$v = \frac{l}{\Delta t} \qquad (5)$$

where, l is the distance between a pair of pick-up coils and Δt is the time difference between the maximum in the induced *emf*.

Results and discussion

Studied Co-rich and Fe-rich as-prepared microwires present rather different magnetic properties and hence GMI effect: i) $Fe_{75}B_9Si_{12}C_4$ microwires present perfectly rectangular hysteresis loops typical for Fe-rich microwires with high and positive magnetostriction coefficient, λ_s, ($\lambda_s \approx 35x10^{-6}$) exhibiting magnetic bistability. However, $Co_{69.2}Fe_{4.1}B_{11.8}Si_{13.8}C_{1.1}$ microwires present linear hysteresis loops previously reported for Co-based glass-coated microwires with low and negative λ_s ($\lambda s \approx -10^{-7}$) [**6, 21**] (see **Fig. 1a** and **Fig. 1b**). Coercivity, H_c, of $Fe_{75}B_9Si_{12}C_4$ microwires (about 55 A/m) is about an order of magnitude higher that of $Co_{69.2}Fe_{4.1}B_{11.8}Si_{13.8}C_{1.1}$ microwires.

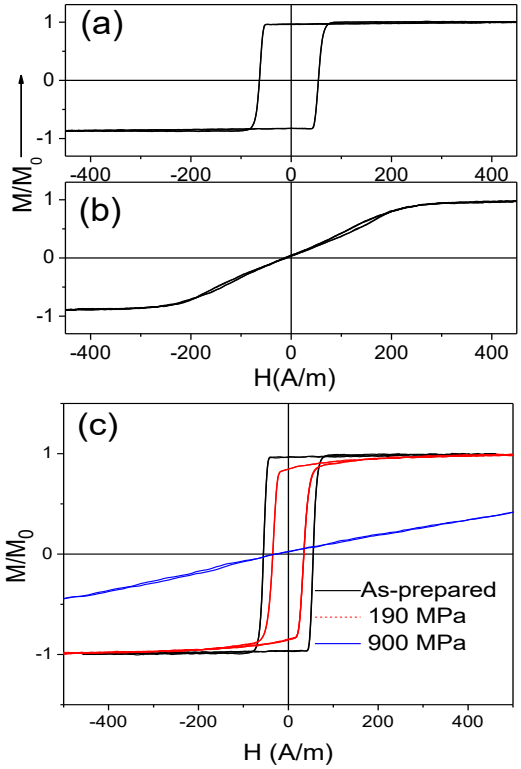

Fig. 1. Hysteresis loops of as-prepared $Fe_{75}B_9Si_{12}C_4$ (a) and (b) $Co_{69.2}Fe_{4.1}B_{11.8}Si_{13.8}C_{1.1}$ microwires. (c) Hysteresis loops of as-prepared and stress-annealed at T_{ann}=300° C (190 and 900 MPa) $Fe_{75}B_9Si_{12}C_4$ microwires.

Accordingly, magnetically softer $Co_{69.2}Fe_{4.1}B_{11.8}Si_{13.8}C_{1.1}$ microwires exhibit an order of magnitude higher GMI ratio than $Fe_{75}B_9Si_{12}C_4$ microwires (**see Fig. 2**).

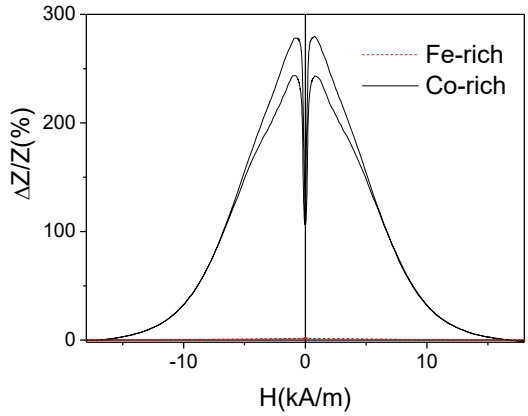

Fig. 2. *ΔZ/Z(H)* dependences of as-prepared $Co_{69.2}Fe_{4.1}B_{11.8}Si_{13.8}C_{1.1}$ and $Fe_{75}B_9Si_{12}C_4$ measured at 100 MHz.

Stress annealing of Fe based microwires allowed considerable magnetic softening (coercivity decreasing) and inducing of transverse magnetic anisotropy as can be observed from hysteresis loops measured in stress-annealed $Fe_{75}B_9Si_{12}C_4$ microwires (**Fig. 1c**). Magnetic properties are considerably affected by the stress, σ_m, applied during the stress annealing: induced transverse magnetic anisotropy becomes more noticeable with increasing of σ_m -values.

Accordingly, remarkable improvement of GMI ratio is observed in stress-annealed $Fe_{75}B_9Si_{12}C_4$ microwires: improvement of $\Delta Z/Z$ –values by an order of magnitude is achieved (**Fig. 3a**).

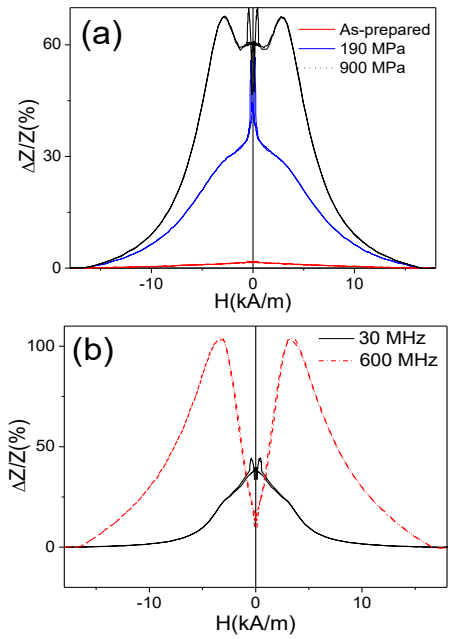

Fig. 3. (a) *ΔZ/Z(H)* dependencies of as-prepared and stress-annealed at T_{ann}=350° C (190 and 900 MPa) $Fe_{75}B_9Si_{12}C_4$ microwires measured at 100 MHz. (b) *ΔZ/Z(H)* dependencies of stress-annealed at T_{ann}=300° C (900 MPa) $Fe_{75}B_9Si_{12}C_4$ microwires measured at 30 and 600 MHz.

Observed *ΔZ/Z(H)* dependencies present irregular shape that can be interpreted as the superposition of double-peak *ΔZ/Z(H)* dependence (more appreciable for the sample stress-annealed under σ_m = 900 MPa) and decay of *ΔZ/Z* with magnetic field, *H*.

It is worth mentioning that for low enough frequency (30 MHz) *ΔZ/Z(H)* dependence of stress-annealed (900 MPa) $Fe_{75}B_9Si_{12}C_4$ microwires presents a maximum at H = 0 (decay of *ΔZ/Z* with magnetic field, *H*). However, at more elevated frequencies (*f* = 600 MHz) a double-peak *ΔZ/Z(H)* dependence is observed (**see Fig. 3b**).

Observed effect of frequency on *ΔZ/Z(H)* dependence can be explained considering frequency dependence of the skin penetration depth, δ, as well as magnetic anisotropy distribution within the metallic nucleus.

It is well established [**20, 33**], that the penetration skin depth decreases with the frequency increasing.

The penetration depth of the AC current, δ, is given by [**2, 3**]:

$$\delta = \left(\pi\sigma \cdot \mu_\phi \cdot f\right)^{-1/2} \quad (6)$$

where σ is the electrical conductivity and μ_ϕ - the circumferential magnetic permeability.

At relatively low frequency of 10 MHz, the skin depth is comparable and even higher than the microwire radius and the current is flowing through the whole ferromagnetic nucleus.

On the other hand, experimentally confirmed [**34-36**] that the magnetic domain structure of magnetic wires consists of outer domain shell with circular magnetization orientation and inner axially magnetized core.

Observed influence of stress-annealing on hysteresis loop of $Fe_{75}B_9Si_{12}C_4$ microwires can be associated with changes of domain structure after stress-annealing.

The inner axially magnetized core radius, R_c, that can be estimated from squireness ratio, M_r/M_s as [**34, 35**]:

$$R_c = R(M_r/M_S)^{1/2} \quad (7)$$

being *R*- microwire radius.

Consequently, from M_r/M_s values we evaluated the dependence of the radius of inner axially magnetized core, R_c, on σ_m. As can be observed from **Fig. 4**, R_c -values progressively decrease with increasing of σ_m -values.

Considering results presented in **Fig. 4** we can explain the observed influence of stress-annealing on *ΔZ/Z(H)* dependencies as following:

For low σ_m -values the volume of the outer domain shell is small (at σ_m =190 MPa R_c is only slightly lower than R). Consequently, stress annealed $Fe_{75}B_9Si_{12}C_4$ (190 MPa) microwire presents predominantly axial anisotropy (as confirmed by **Fig. 3c**). Increasing the σ_m -values the volume of the outer domain shell grows. Therefore, double-peak *ΔZ/Z(H)* dependence becomes more evident (as also confirmed by **Fig. 4**). At elevated frequencies the presence of the circumferential magnetic anisotropy near the surface of metallic nucleus becomes more relevant. Therefore, at elevated frequencies (500 MHz) the double-peak *ΔZ/Z(H)* dependence in stress annealed $Fe_{75}B_9Si_{12}C_4$ (900 MPa) becomes visible.

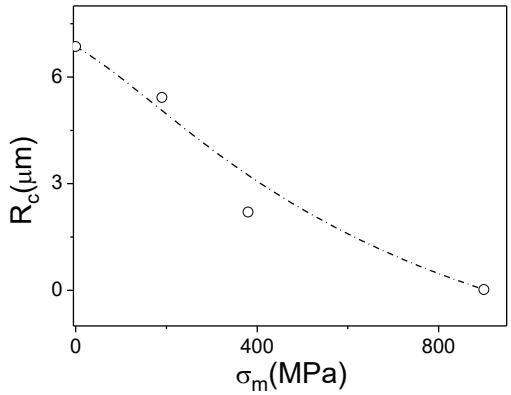

Fig. 4. Dependence of radius of inner axially magnetized core, R_c, on stress applied during the annealing in $Fe_{75}B_9Si_{12}C_4$ microwire.

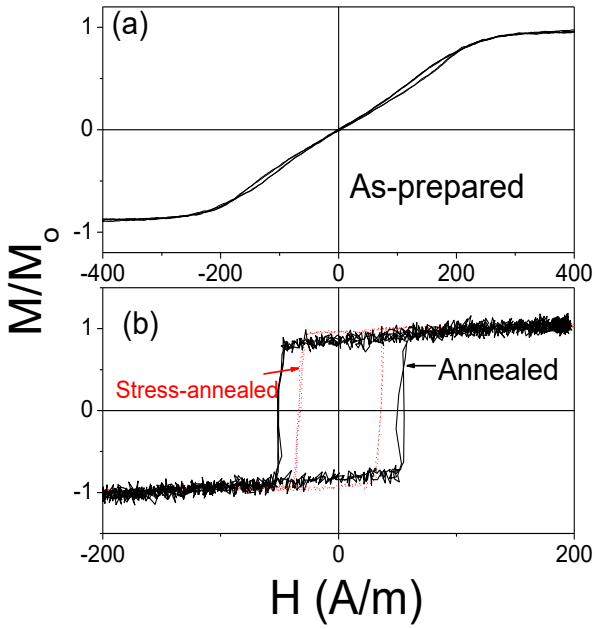

Fig. 5. Hysteresis loops of as-prepared (a) and annealed and stress-annealed ($\sigma_m \approx$ 80 MPa) at 300 °C for 60 min (b) $Co_{69.2}Fe_{4.1}B_{11.8}Si_{13.8}C_{1.1}$ microwires.

Upon annealing the hysteresis loop of Co-rich microwires becomes rectangular presenting considerable magnetic hardening (**see Fig. 5**). However, stress-annealed $Co_{69.2}Fe_{4.1}B_{11.8}Si_{13.8}C_{1.1}$ microwires present lower coercivity as compared to annealed without stress microwires (**see Fig. 5b**). In spite of magnetic hardening and rectangular hysteresis loop stress-annealed $Co_{69.2}Fe_{4.1}B_{11.8}Si_{13.8}C_{1.1}$ microwires still present high GMI effect of the order of 200% (at 100 MHz, **see Fig. 6**).

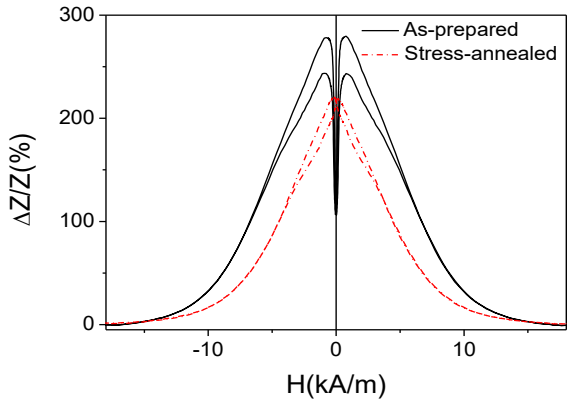

Fig. 6. Comparison of *ΔZ/Z (H)* dependencies of as-prepared and stress-annealed $Co_{69.2}Fe_{4.1}B_{11.8}Si_{13.8}C_{1.1}$ microwire (T_{ann} = 300 ^{0}C, t_{ann} = 5 min, σ_m = 80 MPa).

Hysteresis loops of Co-rich microwires observed after stress-annealing present features similar to that of Fe-rich microwires and annealed Co-rich microwires, i.e. rectangular shape that must be related to presence of single and large Barkhausen jump and induced magnetic bistability. Therefore, similarly to annealed without stress Co-rich microwires [**37**] stress-annealed $Co_{69.2}Fe_{4.1}B_{11.8}Si_{13.8}C_{1.1}$ microwires present single domain wall (DW) propagation. From **Fig. 7** we can observe that similarly to $Fe_{75}B_9Si_{12}C_4$ microwire stress-annealed $Co_{69.2}Fe_{4.1}B_{11.8}Si_{13.8}C_{1.1}$ microwires present linear dependence of DW velocity, *v*, on magnetic field, H (**see Fig. 7**). However, *v*-values observed in stress-annealed $Co_{69.2}Fe_{4.1}B_{11.8}Si_{13.8}C_{1.1}$ microwires at the same H-values are almost twice superior to $Fe_{75}B_9Si_{12}C_4$ microwire (**Fig. 7**).

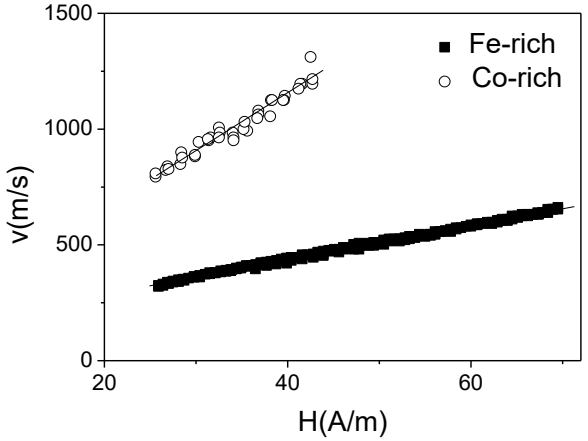

Fig. 7. *v(H)* dependencies of as-prepared $Fe_{75}B_9Si_{12}C_4$ and stress-annealed (T_{ann} = 300 ^{0}C, t_{ann} = 60 min, σ_m = 80 MPa) $Co_{69.2}Fe_{4.1}B_{11.8}Si_{13.8}C_{1.1}$ microwires.

Consequently, stress annealing of ferromagnetic microwires allows achievement of interesting combination of magnetic properties. In the Fe-rich microwires stress-annealing allows remarkable improvement of magnetic softness and GMI effect. Stress-annealed Co-rich microwires can simultaneously present single and fast domain wall (DW) propagation and high GMI effect.

The origin of stress-induced anisotropy in amorphous materials is previously discussed in terms of either "back stresses" or directional pair ordering [**28-30, 38, 39**].

Generally, pair ordering mechanism is assumed for amorphous alloys with two or more magnetic elements. Since one of studied microwire ($Fe_{75}B_9Si_{12}C_4$) contains only one transition metal we consider that the back stresses mechanism of stress-induced anisotropy is more probable.

It is worth mentioning that previously GMI effect has been studied in various soft magnetic materials [**1, 18, 20, 21, 27, 32, 40-44**]. The comparison summarizing the previous achievements on GMI effect of magnetic materials is provided in **Table 1**.

Table 1. Summary of the previous literatures on Giant Magneto-Impedance effect of magnetic materials.

Magnetic materials / preparation method	**Maximum GMI ratio, $\Delta Z/Z_{max}$ (%)**	**Source**
Crystalline, mumetal wire/ annealed	40	[1]
Amorphous, Co-rich wire/in-rotating water	350	[18]
Amorphous, Co-rich wire/melt extracted	450	[40]
Co-rich/sputtered thin films, filed annealed	40	[41]
Amorphous Co-rich, glass-coated microwire/Taylor-Ulitovsky, Joule heated	600	[20]
Amorphous Co-rich, glass-coated microwire/ Taylor-Ulitovsky, as-prepared	615	[21]
Amorphous Co-rich, glass-coated microwire/Taylor-Ulitovsky, Joule heated	650	[42]
Nanocrystalline Fe-rich wires/in-rotating water, annealed	120	[43]
Nanocrystalline Fe-rich,glass-coated microwire/Taylor-Ulitovsky, annealed	125	[27]
Amorphous Fe-Ni rich glass-coated microwire/Taylor-Ulitovsky, annealed	45	[44]
Amorphous Fe-rich glass-coated microwire/Taylor-Ulitovsky, as-prepared	30	[32]
Amorphous Fe-rich glass-coated microwire/Taylor-Ulitovsky, stress-annealed	125	[32]

As can be appreciated from provided above comparison of the previous achievements on GMI effect the highest GMI ratios are achieved for amorphous magnetically soft wires. Additionally, the

appropriate post-processing is a useful tool for GMI effect optimization.

Conclusion

We observed that the stress-annealing allows remarkable improvement of GMI effect in Fe-rich microwires and observation of unique combination of magnetic properties in Co-rich microwires: simultaneous observation of single domain wall propagation and still high GMI effect in Co-rich microwires. An order of magnitude GMI ratio and magnetic softness improvement in Fe-rich microwires is demonstrated.

Influence of frequency on $\Delta Z/Z(H)$ dependence in stress-annealed Fe-rich microwires has been explained considering frequency dependence of the skin penetration depth, δ, as well as magnetic anisotropy distribution within the metallic nucleus.

For interpretation of observed effect of stress annealing we considered internal stresses relaxation after annealing and interplay of compressive "back-stresses" arising after stress annealing and axial internal stresses and change of the spatial distribution of the magnetic anisotropy and hence the domain structure inside the microwire and near the surface.

The future scope of our research will be focused on magnetic wires miniaturization and further development of appropriate post-processing.

Acknowledgements

This work was supported by Spanish MINECO under MAT2013-47231-C2-1-P and by the Government of the Basque Country under the scheme of "Ayuda a Grupos Consolidados" (Ref.: IT954- 16), PIBA 2018-44 and Elkartek (RTM 4.0) projects. The authors thank for technical and human support provided by SGIker of UPV/EHU (Medidas Magneticas Gipuzkoa) and European funding (ERDF and ESF).

Author's contributions

Conceived the plan: AZ, JG, VZ; Sample preparation: VZ; Performed the experiments: PCL, LGG, JMB, MI; Data analysis: AZ, PCL, LGG; Wrote the paper: AZ. Authors have no competing financial interests.

References

1. Harrison, E. P.; Turney, G. L.; Rowe, H., *Nature*, **1935,** *135*, 961. **DOI:** 10.1038/135961a0
2. Panina, L. V.; Mohri, K., *Appl. Phys. Lett.*, **1994**, *65***,** 1189. **DOI:** 10.1063/1.112104
3. Beach, R.; Berkowitz, A., *Appl. Phys. Lett.*, **1994**, *64*, 3652. **DOI:** 10.1063/1.111170
4. Zhukova, V.; Blanco, J. M.; Rodionova, V.; Ipatov, M.; Zhukov, A., *J. Appl. Phys.*, **2012**, *111*, 07E311. **DOI:** 10.1063/1.3672076
5. Phan, M. H.; Peng, H. X., *Prog. Mater. Sci.*, **2008,** *53*, 323. **DOI:** 10.1016/j.pmatsci.2007.05.003
6. Zhukov, A.; Ipatov, M.; Zhukova, V., Advances in Giant Magnetoimpedance of Materials, in Handbook of Magnetic Materials; Buschow K.H.J. (Ed.), Elsevier**:** North Holland, **2015**, *24*, 139. **DOI:** 9780444636416
7. Mohri, K.; Uchiyama, T.; Shen, L. P.; Cai C. M.; Panina, L. V., *J. Magn. Magn. Mater.*, **2002**, *249*, 351. **DOI:** 10.1016/S0304-8853(02)00558-9
8. Cobeño, A. F.; Zhukov, A.; Blanco J. M.; Larin, V.; Gonzalez, J., *Sens. Actuators, A*, **2001**, *91*, 95. **DOI:** 10.1016/S0924-4247(01)00502-7
9. Hauser, M.; Kraus, L.; Ripka, R., *IEEE Instrum. Meas. Magazine*, **2001**, *4*, 28. **DOI:** 10.1109/5289.930983
10. Zhukov, A.; Ipatov, M.; Talaat, A.; Blanco, J. M.; Hernando, B.; Gonzalez-Legarreta, L.; Suñol, J. J.; Zhukova, V., *Crystals*, **2017**, *7*, 41. **DOI:** 10.3390/cryst7020041
11. Gudoshnikov, S.; Usov, N.; Nozdrin, A.; Ipatov, M.; Zhukov, A.; Zhukova, V., *Phys. Status Solidi. A*, **2014**, *211*, 980. **DOI:** 10.1002/pssa.201300717
12. Ding, L.; Saez, S.; Dolabdjian, C.; Melo, L. G. C.; Yelon, A.; Ménard, D., *IEEE Sens. J*, **2009**, *9*, 159. **DOI:** 10.1109/JSEN.2008.2011067
13. Zhukov, A.; Cobeño, A.F.; Gonzalez, J.; Blanco, J. M.; Aragoneses, P.; Dominguez, L., *Sens. Actuators, A*, **2000**, *81*, 129. **DOI:** 10.1016/S0924-4247(99)00152-1
14. Talaat, A.; Alonso, J.; Zhukova, V.; Garaio, E.; García J. A.; Srikanth H.; Phan, M. H.; Zhukov, A., *Sci. Rep.*, **2016**, *6*, 39300. **DOI:** 10.1038/srep39300
15. Malátek, M.; Kraus, L., *Sens. Actuators, A*, **2010**, *164*, 41. **DOI:** 10.1016/j.sna.2010.09.011
16. Zhou, H.; Panand, Z.; Zhang, D., *Sensors*, **2017**, *17*, 1103. **DOI:** 10.3390/s17051103
17. Gemperle, R.; Kraus, L.; Schneider, J., *Czezh. J. Phys. B*, **1978**, *28*, 1138. **DOI:**10.1007/BF01602803
18. Blanco, J. M.; Zhukov, A. P.; A., Gonzalez, J., *J. Phys. D:Appl. Phys.*, **1999**, 32, 3140. **DOI:** 10.1088/0022-3727/32/24/308
19. Zhukov, A.; Ipatov, M.; Churyukanova, M.; Talaat, A.; Blanco, J. M.; Zhukova, V., *J. Alloys Compd.*, **2017,** *727*, 887. **DOI:** 10.1016/j.jallcom.2017.08.119
20. Pirota, K. R.; Kraus, L.; Chiriac, H.; Knobel, M., *J. Magn. Magn. Mater.*, **2000**, *21*, L243. **DOI:** 10.1016/S0304-8853(00)00554-0
21. Zhukov, A.; Zhukova, V.; Blanco, J. M.; Gonzalez, J., *J. Magn. Magn. Mater.*, **2005**, *294*, 182. **DOI:** 10.1016/j.jmmm.2005.03.033
22. Antonov, A. S.; Borisov, V. T.; Borisov, O. V.; Prokoshin, A. F.; Usov, N. A., *J. Phys. D: Appl. Phys.*, **2000**, *33*, 1161. **DOI:** 10.1088/0022-3727/33/10/305
23. Chiriac, H.; Ovari, T. A.; Pop, Gh., *Phys. Rev. B*, **1995**, *42*, 10105. **DOI:** 10.1103/PhysRevB.52.10104
24. Zhukov, A.; Gonzalez, J.; Torcunov, A.; Pina, E.; Prieto, M. J.; Cobeño, A. F.; Blanco, J. M.; Larin, V.; Baranov, S., *J. Magn. Magn. Mater.*, **1999**, *203*, 238. **DOI:** 10.1016/S0304-8853(99)00240-1
25. Eggert, R.G., *Nat. Chem.*, **2011**, *3*, 688. **DOI:** 10.1038/nchem.1116
26. Zhukov, A. P.; Talaat, A.; Ipatov, M.; Blanco, J. M.; Gonzalez-Legarreta, L.; Hernando, B.; Zhukova, V., *IEEE Trans. Magn.*, **2014**, *50*, 2501905. **DOI:** 10.1109/TMAG.2014.2303396
27. Talaat, A.; Zhukova, V.; Ipatov, M.; del Val J. J.; Blanco, J. M.; Gonzalez-Legarreta, L.; Hernando, B.; Churyukanova, M.; Zhukov, A., *JOM*, **2016**, *68*, 1563. **DOI:** 10.1007/s11837-016-1889-y
28. Zhukov, A.; Zhukova, V.; Larin, V.; Blanco, J. M.; Gonzalez, J., *Phys. B*, **2006**, *384*, 1. **DOI:** 10.1016/j.physb.2006.05.018
29. Zhukova, V.; Ipatov, M.; Talaat, A.; Blanco, J. M.; Churyukanova, M.; Zhukov, A., *J. Alloys Compd.*, **2017**, *707*, 189. **DOI:** 10.1016/j.jallcom.2016.10.178
30. Zhukova, V.; Blanco, J. M.; Ipatov, M.; Gonzalez, J.; Churyukanova, M.; Zhukov, A., *Scr. Mater.*, **2018**, *142*, 10. **DOI:** 10.1016/j.scriptamat.2017.08.014
31. Beato-López, J. J.; Vargas-Silva, G.; Pérez-Landazábal, J. I.; Gómez-Polo, C., *Sens. Actuators, A*, **2018,** *269*, 269. **DOI:** 10.1016/j.sna.2017.11.040

32. Zhukov, A.; Talaat, A.; Ipatov, M.; Zhukova, V., *IEEE Magn. Lett.*, **2015**, *6*, 2500104.
DOI: 10.1109/LMAG.2015.2397877
33. Lachowicz, H.; García, K. L.; Kuzminski, M.; Zhukov, A.; Vazquez, M., *Sens. Actuators, A*, **2005**, *119*, 384.
DOI: 10.1016/j.sna.2004.10.017
34. Vázquez, M.; Chen, D. X., *IEEE Trans. Magn.*, **1995**, *31*, 1229.
DOI: 10.1109/20.364813
35. Zhukova, V.; Blanco, J. M.; Ipatov, M.; Churyukanova, M.; Taskaev, S.; Zhukov, A., *Sci. Rep.*, **2018**, *8*, 3202.
DOI: :10.1038/s41598-018-21356-3
36. Zhukova, V.; Blanco, J.M.; Ipatov, M.; Zhukov, A., *J. Appl. Phys.*, **2009**, *106*, 113914.
DOI: 10.1063/1.3266009
37. Zhukov, A.; Talaat, A.; Ipatov, M.; Blanco, J. M.; Zhukova, V., *J. Alloys Compd.*, **2014**, *615*, 610**.**
DOI: 10.1016/j.jallcom.2014.07.079
38. Luborsky, F. E.; Walter, J. L., *IEEE Trans. Magn.*, **1977,** *13*, 953.
DOI: 10.1109/TMAG.1977.1059494
39. Haimovich, J.; Jagielinski, T.; Egami, T., *J. Appl. Phys.*, **1985**, *57*, 3581.
DOI: 10.1063/1.335013
40. Jiang, S. D.; Eggers, T.; Thiabgoh, O.; Xing, D. W.; Fei, W. D.; Shen, H. X.; Liu, J. S.; Zhang, J. R.; Fang, W. B.; Sun, J. F.; Srikanth H., Phan; M. H., *Sci. Rep.*, **2017**, *7*, 46253.
DOI: 10.1038/srep46253
41. Panina, L V. **:** Mohri, K. ; Uchyama, T.; Noda, M. ; Bushida. K., *IEEE Trans. Magn.* **1995**, *31*, 1249.
DOI: 10.1109/20.364815
42. Corte-León, P.; Zhukova, V.; Ipatov, M.; Blanco, J.M.; González. J.; Zhukov, A., *IEEE Trans. Magn.* **2018**, *55*.
DOI: 10.1109/TMAG.2018.2868895
43. Knobel, M.; Sánchez, M. L.; Gómez-Polo, C.; Marín, P.; Vázquez, M.; Hernando, A., *J. Appl. Phys.*, **1996**, *79*, 1646.
DOI: 10.1063/1.361009
44. Zhukov, A.; Churyukanova, M.; Kaloshkin, S.; Semenkova, V.; Gudoshnikov, S.; Ipatov, M.; Talaat, A.; Blanco, J. M.; Zhukova, V., *J. Alloys Compd.*, **2015**, *651*, 718.
DOI: 10.1016/j.jallcom.2015.08.151

